Integral Backstepping-based Nonlinear Flight Control Strategy for Quadrotor Aerial Robot with Unknown Mass

Jin Wang
Zhejiang University
Room 416, 5th Teaching Buildings, No.38 Zheda road, Xihu district, Hangzhou, Zhejiang province
+86-18657118082
21624027@zju.edu.cn

Zhou Fang
Zhejiang University
Room 416, 5th Teaching Buildings, No.38 Zheda road, Xihu district, Hangzhou, Zhejiang province
+86-13116747300
zfang@zju.edu.cn

Wenjie Zhao
Zhejiang University
Room 416, 5th Teaching Buildings, No.38 Zheda road, Xihu district, Hangzhou, Zhejiang province
+86-13588741633
zhaowenjie8@zju.edu.cn

ABSTRACT
This paper aims at obtaining a stable and rapid-responsive controller for quadrotor aerial robots with unknown or changeable mass. Based on Newton-Euler formula, integral backstepping method and fractional-order PI/PD control, an adaptive flight control strategy is carried out in Matlab with Lyapunov stability theorem to ensure its stability. The control strategy includes cascade fractional PI/PD control for rotational loop and integral backstepping control for translational loop. Through the comparison with conventional PID flight controller, main criteria for performance as setting time, maximum overshoot and steady-error show its improvement. After validating the proposed control system and controller tuning with several meta-heuristic algorithms, results from non-linear simulation verify the effectiveness and robustness for hovering or near hovering (near quasi-stationary) flight of quadrotors.

CCS Concepts
Computing methodologies → Artificial intelligence → Control methods → Computational control theory

Keywords
Fractional-order PI/PD; Integral backstepping; Unknown mass quadrotor control.

1. INTRODUCTION
The study on quadrotor flying robots has drawn increasing attentions in recent decades, for their extensive applications on both military and entertainment fields. The quadrotors have 6-DOF (degrees of freedom): three position parameters (x, y, z) and three attitude variables (roll/φ, pitch/θ, yaw/ψ), However, only four control signals (i.e., the main thrust, rolling, pitching, and yaw torques) are involved to control the movement, which increases the difficulty of constructing a stable real-time controller for quadrotor aerial robots with features as nonlinear, strong coupling and under-actuated.

ICRCA '18, August 11–13, 2018, Chengdu, China

ACM ISBN 978-1-4503-6530-7/18/08…$15.00
https://doi.org/10.1145/3265639.3265654

Numerous control methods have been developed and implemented on quadrotor flight control to reach optimal stability and reliability. Samir Bouabdallah et al. purposed an integral backstepping control of quadrotor and realized its accurate control for taking-off, altitude and position [1]. Ye Wang et al. presented a predictive nonlinear control method with constraint conditions for quadrotors [2].Yanmin Chen et al. addressed a decentralized Proportional-Integral-Derivative (PID) neural network control for quadrotor to improve the robustness in windy situation [3].

The flight control system of quadrotors is always divided into two loops, the outer and the inner ones; and they govern translational and attitude motion respectively. PID is the most commonly used method in aircraft control. In this study, instead of using conventional PID controller, a cascade Fractional-Order PI/PD (FOPI/PD) controller is introduced in the inner loop to improve the accuracy. For the outer loop, the integral backstepping controller is implemented to cope with nonlinear dynamics.

In this paper, a situation requiring quadrotors to convey and unload weights is considered. For instance, the mass of an agricultural Unmanned Aerial Vehicle (UAV) is continuously decreasing while spraying pesticide; when UAVs are used to send relief to disaster regions, the mass of robots varies abruptly. In these kinds of circumstances, the change or uncertainty of mass would impact the forces and moments acting on these robots. In order to obtain more precise altitude information, an adaptive algorithm is implemented for mass estimation.

The main contribution of this paper is implementing cascade FOPID controllers into attitude control of quadrotors and integral backstepping method with mass estimation into position control in order to optimally control the quadrotor with changeable or unknown mass, the controller tuning is realized with several meta-heuristic optimization algorithms.

The rest of this article is arranged as follows: the dynamic model is analyzed in Section 2, the proposed control method and the estimation for mass are presented in Section 3 and Section 4. Section 5 studies the accuracy of the proposed method and the simulation results. At the end, Section 6 summarizes this paper.

2. QUADROTOR DYNAMIC MODEL
In order to better describe the dynamics of aircrafts, the body and inertial coordinate system with Euler angles (as Fig.1) is usually employed. Whereas the Newton's second law only applies in inertial coordinate system, the Direction Cosine Matrix (DCM) is

introduced in Eq.(1), where c(η) and s(η) represents cos(η) and sin(η) respectively.

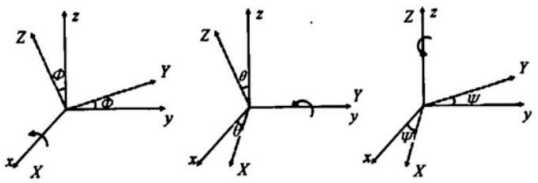

Figure 1. Euler angles.

$$\mathrm{R}=\begin{bmatrix}\cos\psi & 0 & -\sin\psi\\ 0 & 1 & 0\\ \sin\psi & 0 & \cos\psi\end{bmatrix}\begin{bmatrix}1 & 0 & 0\\ 0 & \cos\phi & \sin\phi\\ 0 & -\sin\phi & \cos\phi\end{bmatrix}\begin{bmatrix}\cos\theta & \sin\theta & 0\\ -\sin\theta & \cos\theta & 0\\ 0 & 0 & 1\end{bmatrix} \quad (1)$$
$$=\begin{bmatrix}c(\theta)c(\psi) & c(\theta)s(\psi) & -s(\theta)\\ s(\phi)s(\theta)c(\psi)-c(\phi)s(\psi) & s(\phi)s(\theta)s(\psi)+c(\phi)c(\psi) & s(\phi)c(\theta)\\ c(\phi)s(\theta)c(\psi)+s(\phi)s(\psi) & c(\phi)s(\theta)s(\psi)-s(\phi)c(\psi) & c(\phi)c(\theta)\end{bmatrix}$$

The dynamic equation on the basis of Newton's second law of motion is shown in Eq.(2), a force analysis considering thrust, resistance and gravity is carried out:

$$\mathrm{F}=m\frac{dv}{dt},\mathrm{M}=\frac{dH}{dt} \quad (2)$$

Then on inertial axes, the translational dynamics of quadrotors can be obtained by overleaping the effect of body torques on translational dynamics:

$$\begin{cases} m\ddot{x}=(sin\theta cos\phi cos\psi+sin\phi sin\psi)\sum_{i=1}^{4}\mathrm{F}_i-K_{dx}\dot{x}\\ m\ddot{y}=(sin\theta cos\phi\sin\psi-sin\phi\cos\psi)\sum_{i=1}^{4}\mathrm{F}_i-K_{dy}\dot{y}\\ m\ddot{z}=cos\phi\cos\theta\sum_{i=1}^{4}\mathrm{F}_i-K_{dz}\dot{z}-mg \end{cases} \quad (3)$$

where Fi (i = 1, 2, 3, 4) represents the thrust force produced by each propeller and K_{dx}, K_{dy}, K_{dz} are the aerodynamic coefficients.

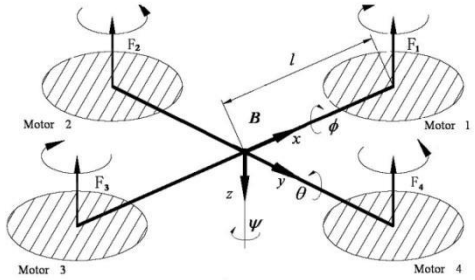

Figure 2. Forces and moments acting on quadrotor.

Considering that the tensor of inertia is homogeneous and the quadrotor is symmetrical as depicted in Fig.2, Eq.(4) derives the relation between Euler angles and the angular velocities of quadrotor.

$$\begin{bmatrix}\dot{\phi}\\ \dot{\theta}\\ \dot{\psi}\end{bmatrix}=\begin{bmatrix}1 & \tan\theta\sin\phi & \tan\theta\cos\phi\\ 0 & \cos\phi & -\sin\phi\\ 0 & \frac{\sin\phi}{\cos\theta} & \frac{\cos\phi}{\cos\theta}\end{bmatrix}\begin{bmatrix}p\\ q\\ r\end{bmatrix} \quad (4)$$

Due to the effect of moments, quadrotor aerial robots will rotate about its center of mass, the moment equations are represented as Eq.(5).

$$\sum M_{\mathrm{b}}=I\dot{W}_b+W_b\times(IW_b)=\begin{bmatrix}I_x\dot{p}+(I_z-I_y)qr\\ I_y\dot{q}+(I_x-I_z)pr\\ I_z\dot{r}+(I_y-I_x)pq\end{bmatrix} \quad (5)$$

where I is the inertial matrix and W=[p q r] represents the body angular velocities on X, Y and Z axis.

While assuming the aerodynamic lift and drag coefficient, denoted as b and d respectively, the drag and thrust for each motor are proportional to its rotating speed:

$$\mathrm{D}_i=d\Omega_i^2,\ \mathrm{F}_i=b\Omega_i^2 \quad (6)$$

The lift force moments on three axis $(M_{T_x}, M_{T_y}, M_{T_z})$ can be deduced as below with l represents the wheelbase:

$$\begin{bmatrix}\mathrm{M}_{Tx}\\ \mathrm{M}_{Ty}\\ \mathrm{M}_{Tz}\end{bmatrix}=\begin{bmatrix}l(\mathrm{F}_4-\mathrm{F}_2)\\ l(\mathrm{F}_3-\mathrm{F}_1)\\ -d\Omega_1^2+d\Omega_2^2-d\Omega_3^2+d\Omega_4^2\end{bmatrix} \quad (7)$$

Moreover, when the two pairs of motors run in different speed, the quadrotor will rotate about Z axis due to the gyroscopic moment:

$$\mathrm{M}_g=\sum_{\mathrm{i}=1}^{4}W^{\mathrm{b}}\times(I_rw_i)=\mathrm{I}_r\begin{bmatrix}-q\\ p\\ 0\end{bmatrix}(-\Omega_1+\Omega_2-\Omega_3+\Omega_4) \quad (8)$$

To obtain a concise model of quadrotor, four invented inputs, denoted as U_1, U_2, U_3 and U_4, are defined [1]:

$$\begin{cases} U_1=\sum_{i=1}^{4}\mathrm{F}_i=b(\Omega_1^2+\Omega_2^2+\Omega_3^2+\Omega_4^2)\\ U_2=l(\mathrm{F}_4-\mathrm{F}_2)=lb(\Omega_4^2-\Omega_2^2)\\ U_3=l(\mathrm{F}_3-\mathrm{F}_1)=(\Omega_3^2-\Omega_1^2)\\ U_4=d(-\Omega_1^2+\Omega_2^2-\Omega_3^2+\Omega_4^2) \end{cases} \quad (9)$$

From Eq.(1-9), the translational and rotational dynamic equations of quadrotor can be expressed as:

$$\begin{cases} \ddot{x} = (\sin\theta\cos\varphi\cos\psi + \sin\varphi\sin\psi)\dfrac{U_1}{m} \\ \ddot{y} = (\sin\theta\cos\varphi\sin\psi - \sin\varphi\sin\psi)\dfrac{U_1}{m} \\ \ddot{z} = \cos\varphi\cos\theta\dfrac{U_1}{m} - g \\ \ddot{\varphi} = \dfrac{I_y - I_z}{I_x}\dot{\theta}\dot{\psi} + \dfrac{U_2}{I_x} \\ \ddot{\theta} = \dfrac{I_z - I_x}{I_y}\dot{\varphi}\dot{\psi} + \dfrac{U_3}{I_y} \\ \ddot{\psi} = \dfrac{I_x - I_y}{I_z}\dot{\varphi}\dot{\theta} + \dfrac{U_4}{I_z} \end{cases} \quad (10)$$

During a hovering flight, the angles are considered as slow dynamics. Therefore, Eq.(10) can be rewritten near the equilibrium point [5]:

$$\begin{cases} \ddot{x} = (\sin\theta\cos\varphi\cos\psi + \sin\varphi\sin\psi)\dfrac{U_1}{m} = \dfrac{U_x U_1}{m} \\ \ddot{y} = (\sin\theta\cos\varphi\sin\psi - \sin\varphi\sin\psi)\dfrac{U_1}{m} = \dfrac{U_y U_1}{m} \\ \ddot{z} = \cos\varphi\cos\theta\dfrac{U_1}{m} - g \\ \ddot{\varphi} = \dfrac{U_2}{I_x} \\ \ddot{\theta} = \dfrac{U_3}{I_y} \\ \ddot{\psi} = \dfrac{U_4}{I_z} \end{cases} \quad (11)$$

3. CONTROL STRATEGY

3.1 Attitude Control

The classical PID controller has been extensively used in varied industrial fields owing to its simplicity and adaptability. Since the development of classical calculus, the idea of fractional calculus has been developed and a half-order derivative was first referenced in 1695 [6]. The differential and transfer functions of FOPID controller are given by:

$$\begin{cases} u(t) = k_p e(t) + k_i D_t^{-\lambda} e(t) + k_d D_t^{\mu} e(t) \\ G_c(s) = k_p + \dfrac{k_i}{s^{\lambda}} + k_d s^{\mu} \ (\lambda, \mu > 0) \end{cases} \quad (12)$$

Where μ and λ are both positive variables, μ is order of differential and λ is the order of integral.

Fraction-order controller leads to better result compared to integral-order controller due to the two additional positive fractional exponential coefficients λ and μ (commonly between 0 to 2). However, only a few researchers have implemented it into quadrotor flight control, the absence of solution methods for fractional differential equation is the primary problem, which has already been solved with lots of methods newly published, including neural network, meta-heuristic algorithms and genetic algorithms, etc. The design of controller becomes more flexible because of the extension of integration and derivation order from integral to non-integral. P.R. Hemavathy and U. Sabura Banu used Genetic Algorithm to tune FOPI cascade control system and controlled the flow of fluid in pipelines [7]. Abhilash K.S. et al. designed a wire-brake system for sport motorcycles with cascade fractional-order control [8].

In this paper, as demonstrated in Fig.3, a cascade control system is applied in attitude control, it contains with two control loops: the FOPI controller as the outer primary controller and the FOPD controller as the inner secondary controller.

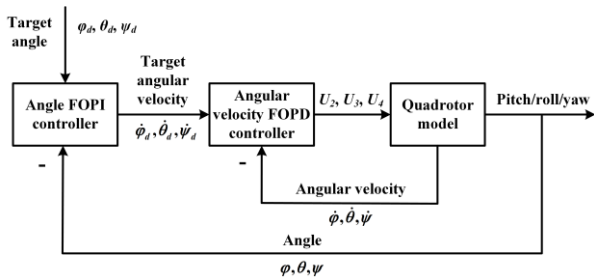

Figure 3. Attitude controller.

Compared with conventional PID control system, cascade control system can enhance robustness and stability because more variables are getting involved. Several meta-heuristic algorithms, including the Artificial Bee Colony (ABC), Grey Wolf Optimization (GWO), Cuckoo Search (CS), Moth Swarm Algorithm (MSA) and Modified Flower Pollination Algorithm (MFPA), etc. are used to select the optimal gain of the FOPI/PD controller, and the main criterion is the best value of the Integral of Time multiply Absolute (ITAE) error. The optimization methodology is explained in Fig.4.

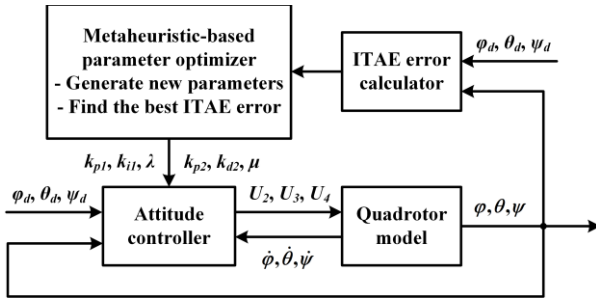

Figure 4. Fractional-order parameters tuning methodology.

3.2 Position Control

In Eq.(11), the position subsystem of quadrotors is presented, as this study concerns about the disturbances of surroundings and uncertainty of variables, a parameter *D* is introduced referring to such disturbances. Afterwards, an integral backstepping control method is implemented to achieve the nonlinear position control and to compensate *D* in three position directions (D_x, D_y and D_z).

In altitude subsystem, the dynamics of quadrotor on the *z*-axis is:

$$m\ddot{z} = \cos\varphi\cos\theta U_1 - mg + D_z \quad (13)$$

Considering a state vector *X* of 12 elements derived as Eq.(14) in order to simplify the analysis:

$$\begin{aligned} x_1 &= \phi \quad & x_7 &= z \\ x_2 &= \dot{\phi} \quad & x_8 &= \dot{z} \\ x_3 &= \theta \quad & x_9 &= x \\ x_4 &= \dot{\theta} \quad & x_{10} &= \dot{x} \\ x_5 &= \psi \quad & x_{11} &= y \\ x_6 &= \dot{\psi} \quad & x_{12} &= \dot{y} \end{aligned} \tag{14}$$

Eq.(13) can be rewritten into state equation form:

$$\begin{cases} \dot{x}_7 = x_8 \\ \dot{x}_8 = \dfrac{1}{m}\left(\cos x_3 \cos x_1 U_1 - mg + D_z\right) \end{cases} \tag{15}$$

The altitude tracking error and rate error are defined as:

$$\begin{aligned} z_7 &= x_{7d} - x_7 \\ z_8 &= \alpha_7 - x_8 \end{aligned} \tag{16}$$

where x_{7d} represents the desired altitude and α_7 is an invented control variable.

The first step is to design the subsystem of z_7 , where

$$\dot{z}_7 = \dot{x}_{7d} - \dot{x}_7 = \dot{x}_{7d} - x_8 \tag{17}$$

To eliminate the steady-error, the virtual input α_7 with integral action is chosen as:

$$\alpha_7 = \dot{x}_{7d} + c_7 z_7 + \sigma_z p_7 \left(c_7, \sigma_z > 0\right) \tag{18}$$

Where $p_7 = \int z_7(\tau) d\tau$, σ_7 is the integral constant.

Combining Eq.(16) with Eq.(17), the derivative of the tracking and rate errors are deduced:

$$\begin{aligned} \dot{z}_7 &= z_8 - c_7 z_7 - \sigma_z p_7 \\ \dot{z}_8 &= -\dot{x}_8 + \ddot{x}_{7d} + c_7 \dot{z}_7 + \sigma_z \dot{p}_7 \end{aligned} \tag{19}$$

The Lyapunov function can be chosen as:

$$V_8 = \frac{1}{2} z_7^2 + \frac{1}{2} z_8^2 + \frac{1}{2} \sigma_z p_7^2 \tag{20}$$

Therefore,

$$\begin{aligned} \dot{V}_8 &= z_7 \dot{z}_7 + z_8 \dot{z}_8 + \sigma_z p_7 \dot{p}_7 \\ &= z_8 \dot{z}_8 + z_7 z_8 - c_7 z_7^2 \end{aligned} \tag{21}$$

To asymptotically stabilize the system, $\dot{V}_8$ should be designed as:

$$\dot{V}_8 = -c_7 z_7^2 - c_8 z_8^2 < 0 \left(c_7, c_8 > 0\right) \tag{22}$$

It can be obtained that:

$$\ddot{z}_7 = \dot{z}_8 = -z_7 - c_8 z_8 \tag{23}$$

As U_1 is the only vector that controls the altitude, take Eq.(15) and Eq.(19) into Eq.(23), the U_1 able to ensure the stability of *z7* and *z8* subsystems can be derived as:

$$U_1 = \frac{m}{\cos x_3 \cos x_1}\left[z_7(-c_7^2 + \sigma_z + 1) + z_8(c_7 + c_8) - c_7 \sigma_z p_7 + \ddot{x}_{7d} + g - \frac{D_z}{m} \right] \tag{24}$$

Where c_7, c_8, $\sigma_z > 0$.

Define $\hat{D}_z$ as the estimated value of D_z , $\tilde{D}_z = \hat{D}_z - D_z$ as the estimation error. In order to create the adaptive law of D_z , an extended Lyapunov function is needed:

$$V_8 = \frac{1}{2} z_7^2 + \frac{1}{2} z_8^2 + \frac{1}{2} \sigma_z p_7^2 + \frac{\tilde{D}_z^2}{2m\zeta_z} (\sigma_z, \zeta_z > 0) \tag{25}$$

Taking derivation of Eq.(25):

$$\dot{V}_8 = z_7 z_8 - c_7 z_7^2 + z_8 \dot{\alpha}_7 - z_8 (\dot{x}_8 + \frac{\tilde{D}_z}{m}) + \frac{\tilde{D}_z}{m} (z_8 + \frac{\dot{\tilde{D}}_z}{\zeta_z}) (\zeta_z > 0) \tag{26}$$

Assuming the disturbances are stable over the system stable rising time ($\dot{D}_z = 0$), it is obvious that $\dot{\tilde{D}}_z = \dot{\hat{D}}_z$.

Combine Eq.(15-19) and Eq.(26), by satisfying Eq.(22) to guarantee the stability of z_7 and z_8 subsystems with external disturbances,

$$\begin{cases} \dot{\hat{D}}_z = -\zeta_z z_8 \\ U_1 = \dfrac{m}{\cos x_3 \cos x_1}\left[z_7(-c_7^2 + \sigma_z + 1) + z_8(c_7 + c_8) - c_7 \sigma_z p_7 + \ddot{x}_{7d} + g - \dfrac{\hat{D}_z}{m} \right] \end{cases} \tag{27}$$

where ζz, c7, c8, σ7 > 0.

Similarly, adaptive control vectors and disturbances can be deduced when the integral backstepping method is applied to the horizontal field:

$$\dot{\hat{D}}_x = -\zeta_x z_{10} \quad \dot{\hat{D}}_y = -\zeta_y z_{12} \tag{28}$$

$$\begin{aligned} U_x &= \frac{m}{U_1}\left[z_9(-c_9^2 + \sigma_x + 1) + z_{10}(c_9 + c_{10}) - c_9 \sigma_x p_9 + \ddot{x}_{9d} - \frac{\hat{D}_x}{m} \right] \\ U_y &= \frac{m}{U_1}\left[z_{11}(-c_{11}^2 + \sigma_y + 1) + z_{12}(c_{11} + c_{12}) - c_{11} \sigma_y p_{11} + \ddot{x}_{11d} - \frac{\hat{D}_y}{m} \right] \end{aligned} \tag{29}$$

with the variables $z_9 = x_{9d} - x_9$, $z_{10} = \dot{x}_{9d} + c_9 z_9 + \sigma_9 p_9 - x_{10}$, $z_{11} = x_{11d} - x_{11}$, $z_{12} = \dot{x}_{11d} + c_{11} z_{11} + \sigma_{11} p_{11} - x_{12}$ and ζ_x, ζ_y, c_9, c_{10}, c_{11}, c_{12}, σ_x, $\sigma_y > 0$.

4. ESTIMATOR OF MASS

In backstepping control approach, the control law is designed by using virtual variants, denoted as α, while the derivative order is getting higher (n>3), the calculation would be quite complicated and tedious as the control signal U will include multiple derivative of the virtual variant. In this section, the estimation of mass only requires a single derivation of α, hence there is no need to worry about overly cumbersome analytic calculation.

As the situations mentioned in introduction, the mass m of aircrafts is usually unknown to the controller, while Eq.(11) demonstrates that the value of mass has an essential effect on vertical position performance, in order to obtain better performance, an adaptive methodology is used in this non-linear situation. The estimate $\hat{m}$ would act as variant and converge to the true value m when system is stabilized.

Since the vertical state equation, which is rewritten below, is closely related to *m*, the adaptive rate is calculated based on back-stepping mythology with $\tilde{m} = \hat{m} - m$ defined as the estimation error.

Consider the extended Lyapunov function:

$$V_8 = \frac{1}{2} z_7^2 + \frac{1}{2} z_8^2 + \frac{1}{2} \sigma_z p_7^2 + \frac{\tilde{D}_z^2}{2m\zeta_z} + \frac{\tilde{m}^2}{2m} (\sigma_z, \zeta_z > 0) \quad (30)$$

Take the derivation of V8:

$$\begin{aligned} \dot{V}_8 &= z_7 \dot{z}_7 + z_8 \dot{z}_8 + \sigma_z p_7 z_7 + \frac{\tilde{D}_z \dot{\tilde{D}}_z}{m\zeta_z} + \frac{\tilde{m}\dot{\tilde{m}}}{m} \\ &= z_7 z_8 - c_7 z_7^2 + z_8 \dot{\alpha}_7 - z_8 \left[\dot{x}_8 + \frac{\tilde{D}_z}{m} - \frac{\tilde{m}(\cos x_3 \cos x_1 U_1 + \hat{D}_z)}{m\hat{m}} \right] \\ &+ \frac{\tilde{D}_z}{m} (z_8 + \frac{\dot{\tilde{D}}_z}{\zeta_z}) + \frac{\tilde{m}}{m} \left[\dot{\tilde{m}} - \frac{z_8 (\cos x_3 \cos x_1 U_1 + \hat{D}_z)}{\hat{m}} \right] \\ &= -c_7 z_7^2 + z_8 (z_7 + \dot{\alpha}_7 + \frac{\cos x_3 \cos x_1 U_1 + \hat{D}_z}{\hat{m}} - g) \\ &+ \frac{\tilde{D}_z}{m} (z_8 + \frac{\dot{\tilde{D}}_z}{\zeta_z}) + \frac{\tilde{m}}{m} \left[\dot{\tilde{m}} - \frac{z_8 (\cos x_3 \cos x_1 U_1 - \hat{D}_z)}{\hat{m}} \right] \end{aligned} \quad (31)$$

The control input U1 can be chosen as:

$$U_1 = \frac{\hat{m}}{\cos x_3 \cos x_1} \left[z_7 (-c_7^2 + \sigma_z + 1) + z_8 (c_7 + c_8) - c_7 \sigma_z p_7 + \ddot{x}_{7d} + g - \frac{\hat{D}_z}{\hat{m}} \right] \quad (32)$$

As $\dot{\tilde{m}} = \dot{\hat{m}} - \dot{m}$, assuming the mass of quadrotor varies in a linear rate of a (a=0 if mass is constant or period of air-drop $\Delta T > T_{rise\ time}$ [9]), i.e.

$$\dot{\tilde{m}} = \dot{\hat{m}} - a \quad (33)$$

With the assumption explained in Section 3 ($\dot{\tilde{D}}_z = \dot{\hat{D}}_z$), the adaptive rates $\dot{\hat{m}}$ and $\dot{\hat{D}}_z$ should be designed as:

$$\begin{cases} \dot{\hat{m}} = a + z_8 \begin{bmatrix} z_7 (-c_7^2 + \sigma_z + 1) + z_8 (c_7 + c_8) \\ -c_7 \sigma_z p_7 + \ddot{x}_{7d} + g \end{bmatrix} \\ \dot{\hat{D}}_z = -z_8 \zeta_z \end{cases} \quad (34)$$

with $\zeta_7, c_7, c_8, \sigma_z > 0, \dot{V}_8 = -c_7 z_7^2 - c_8 z_8^2 < 0$.

Until now, the altitude controller is designed as asymptotic stable to cope with unknown/variable mass and vertical disturbances.

5. SIMULATION AND RESULT ANALYSIS

A series of simulations are carried out on Matlab to validate the proposed control system, as well as the advantages compared with classic PID method, the quadrotor control strategy is shown in Fig.5. Some physical parameters of quadrotor used in simulations [10] are demonstrated in Table 1.

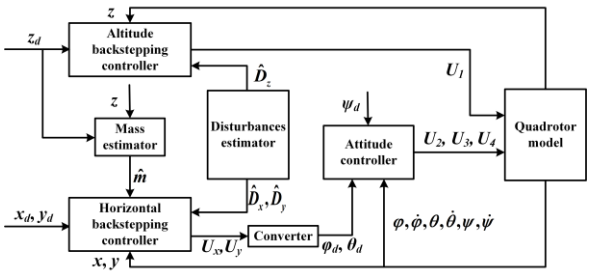

Figure 5. System Control Strategy.

Table 1. Physical parameters of quadrotor

Physical significance	Symbol	Value	Unit
Moment of inertia on *X* axis	I_x	$6.228e^{-3}$	$kg \cdot m^2$
Moment of inertia on *Y* axis	I_y	$6.228e^{-3}$	$kg \cdot m^2$
Moment of inertia on *Z* axis	I_z	$11.21e^{-3}$	$kg \cdot m^2$
Mass(net weight)	*m*	9.0	*kg*
Total mass(full-load)	*m*	25.0	*kg*
Wheel base	*L*	0.232	*m*
Drag coefficient	*b*	$3.13e^{-5}$	$N \cdot s^2$
Resistance coefficient	*d*	$7.5e^{-7}$	$N \cdot ms^2$

Firstly, the total mass of quadrotor is configured as a constant (25kg) and no disturbance is added in order to validate the backstepping strategy for the mass estimation. The results are illustrated in Fig.6. At 5.425s, the estimation of mass is settled and without steady-state error. In Fig.7(a) and (b), comparisons of position and attitude between the proposed method and classic PID is demonstrated. In both controller, the position and altitude converge to the desired coordinate (1,1,1), while the proposed one shows great advantages in setting-time and overshoot.

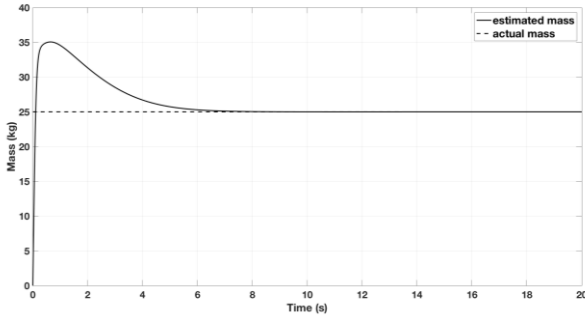

Figure 6. Mass m and its estimation $\hat{m}$.

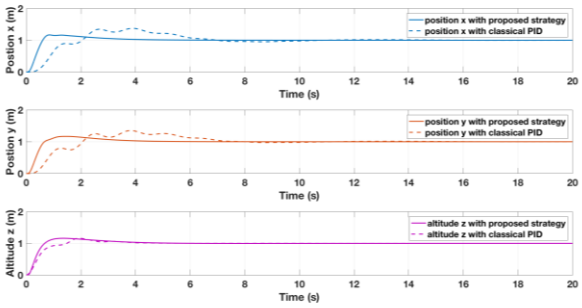

(a) Position x, y and altitude z.

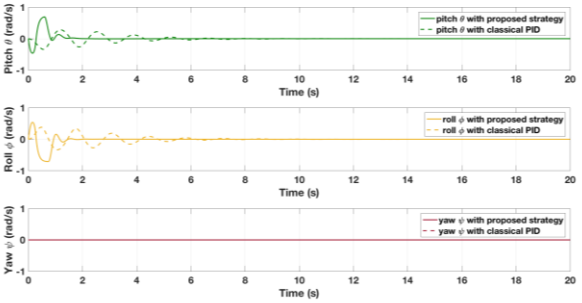

(b) Attitude pitch/θ, roll/φ, yaw/ψ

Figure 7. Simulation results for constant mass.

Afterwards, the mass of quadrotor is set as step-decreasing (2.5kg per 10s for 1.5min) to imitate the airdrop situation. In Fig.8(a), the mass of quadrotor is decreasing according to a step function and the estimated value can follow the track of mass quickly. In Fig.8(b), the effect on altitude is less than 0.01m (1%), however, without mass estimation, classic PID controller cannot maintain z as a constant in the same situation

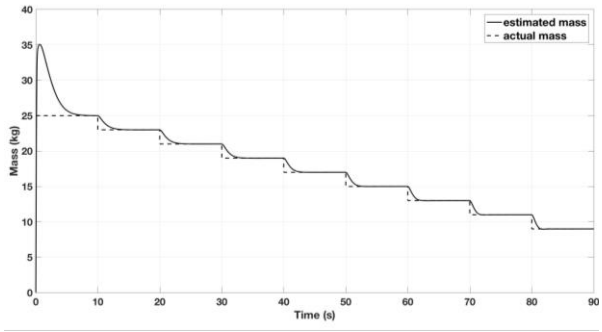

(a) Response curve of $\hat{m}$ in airdrop situation.

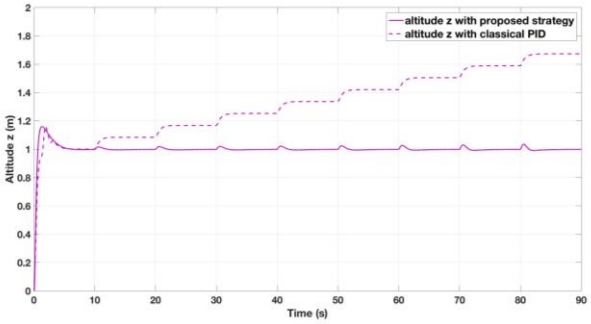

(b) Position x, y and altitude z.

Figure 8. Simulation results for mass changing in step function.

Apart from a step function simulation imitating the airdrop scenario, circumstances requiring high-order mass variation are also taken into consideration. Assuming a quadrotor is assigned to spray pesticide in a certain flow velocity as shown in Fig.9(a), the load changes from 16kg to 0kg in 1.5min(considering the quadrotor weights 9kg), the altitude responses from the proposed controller and classic PID are depicted in Fig.9(b).

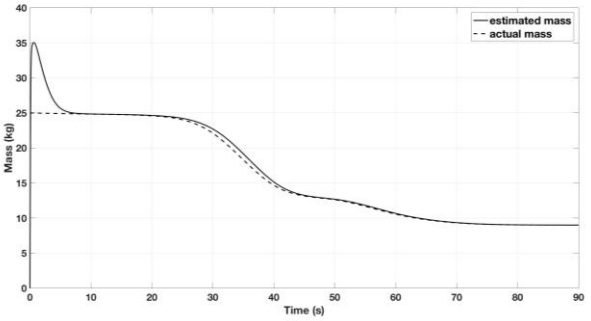

(a) pesticide weight

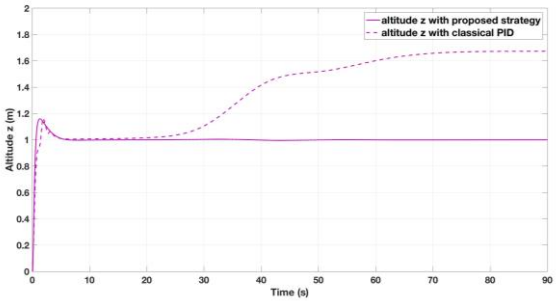

(b) Response curve of altitude z

Figure 9. Simulation results for high-order mass variation.

To verify the robustness of the proposed control strategy, external disturbances are added into the quadrotor system. Random disturbances (amplitude within 0.7m) on three directions are created and removed in sequence. Fig.10 shows that the position controller could compensate the disturbances and reestablish stability easily.

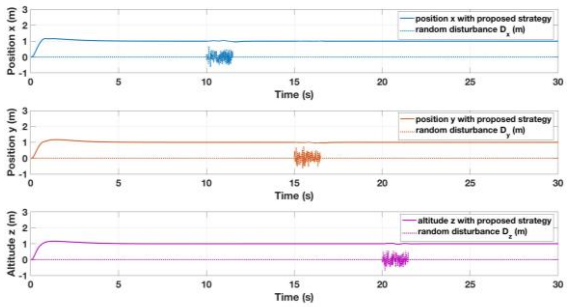

Figure 10. Control response with random disturbances.

In the following simulations, to permit hovering flight, the desired roll angle $\varphi_{d,}$ and pitch angles θ_d are set as zero. In Fig.11(a), a rectangular flight path is given, the response of quadrotor position and altitude control are illustrated based on airdrop situation. In Fig.11(b), a spiral (cylindric) flight path is constructed and the control response is recorded. In both circumstances, the results show that the proposed control system is able to quickly stabilize the quadrotor with unknown or variable mass and various flight paths.

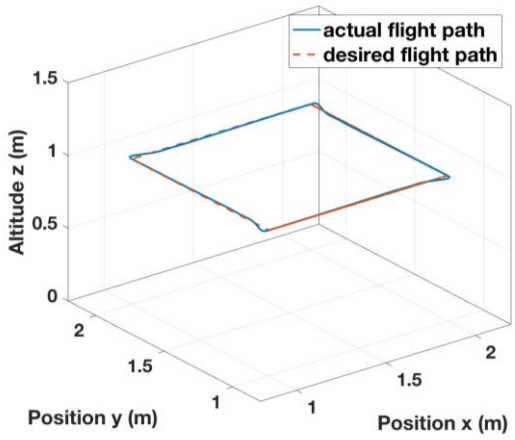

(a) Control response for rectangular flight path.

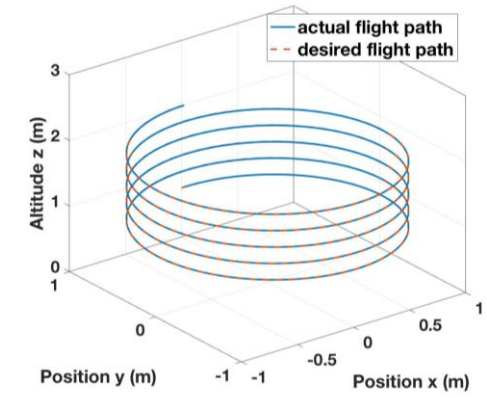

(b) Control response for spiral flight path.

Figure 11. Response curve for various flight paths.

6. CONCLUSION

This paper proposed a nonlinear control method to stabilize quadrotor flying robots with unknown or changeable mass. Firstly, the dynamic model is derived on the basis of Newton-Euler equation, and then an integral backstepping strategy is applied to the position control, as for the rotational loop and mass estimation, a cascade fractional-order PI/PD controller and an adaptive algorithm are implemented respectively. The Capabilities in trajectory tracking, attitude control and mass estimation were examined through the simulations as well as the Lyapunov global stability theorem. Comparison with classic PID method showed the advantages of the proposed method in both position and attitude control, the simulation results illustrated the robustness and effectiveness of the proposed control strategy for quadrotor flying robots.

7. ACKNOWLEDGEMENTS

This work is supported by National Natural Science Foundation (NNSF) of China under Grant 61703366, the Fundamental Research Funds for the Central Universities(2016FZA4023, 2017QN81006), and the Science and Technology department of Zhejiang Province under Grant 2016C33246.

8. REFERENCES

[1] Samir Bouabdallah and Roland Siegwart. 2007. *Full Control of a Quadrotor.* Proceeding of the 2007 IEEE/RSJ International Conference on Intelligent Robots and Systems.

[2] Ye Wang et al. 2017. *Nonlinear Model Predictive Control with Constraint Satisfactions for a Quadcopter.* 13th European Workshop on Advanced Control and Diagnosis.

[3] Chen Yanmin, He Yongling, Zhou Minfeng. 2015. *Decentralized PID Neural Network Control for a Quadrotor Helicopter Subjected to Wind Disturbance.* Central South University Press and Springer-Verlag Berlin Heidelberg.

[4] Ashfaq Ahmad Mian, Mian Ilyas Ahmad and Daobo Wang, 2008. *Backstepping based Nonlinear Flight Control Strategy for 6 DOF Aerial Robo.,* International Conference on Smart Manufacturing Application.

[5] Fu jiahe and LiRui, 2015. *Fractional PID and Backstepping Control for a Small Quadrotor Helicopter.* Proceedings of the 34th Chinese Control Conference.

[6] YangQuan Chen, Ivo Petráš and Dingyu Xue, 2009, *Fractional Order Control – A Tutorial*. American Control Conference.

[7] P. R. Hemavathy, U. Sabura Banu, 2016, *Tuning of Fractional Order PI Controller for Cascade Control System using Genetic Algorithm.* Indian Journal of Science and Technology.

[8] Abhilash K.S, Krishnapriya T Nair. 2016. *Application of Fractional Order Cascade Control to a Brake-By-Wire Actuator for Sport Motorcycles.* International Advanced Research Journal in Science, Engineering and Technology.

[9] Huanye Liu. 2009. *Study and Design of Flight Control Systems for Small Scale Quadrotors.* Shanghai Jiao Tong University.

[10] Bouabdallah S. 2007. *Design and control of quadrotors with application to autonomous flying[D]*. Ecole Polytechnique Federale de Lausanne